ResearchGate

See discussions, stats, and author profiles for this publication at: https://www.researchgate.net/publication/231232456

Quantum-Mechanical and Thermodynamical Study on the (110) and Reconstructed (111) Faces of NaCl Crystals

ARTICLE *in* CRYSTAL GROWTH & DESIGN · MARCH 2009

Impact Factor: 4.89 · DOI: 10.1021/cg801144x

CITATIONS
14

READS
84

3 AUTHORS:

Marco Bruno
Università degli Studi di Torino
84 PUBLICATIONS **704** CITATIONS
SEE PROFILE

Dino Aquilano
Università degli Studi di Torino
190 PUBLICATIONS **992** CITATIONS
SEE PROFILE

Mauro Prencipe
Università degli Studi di Torino
74 PUBLICATIONS **1,116** CITATIONS
SEE PROFILE

Available from: Marco Bruno
Retrieved on: 24 January 2016

CRYSTAL GROWTH & DESIGN

Subscriber access provided by UNIV STUDI DI TORINO

Article

Quantum-Mechanical and Thermodynamical Study on the (110) and Reconstructed (111) Faces of NaCl Crystals

Marco Bruno, Dino Aquilano, and Mauro Prencipe

Cryst. Growth Des., **2009**, 9 (4), 1912-1916• DOI: 10.1021/cg801144x • Publication Date (Web): 10 February 2009

Downloaded from http://pubs.acs.org on April 1, 2009

Equilibrium shape of a NaCl crystal in pure aqueous solution at T = 300 K

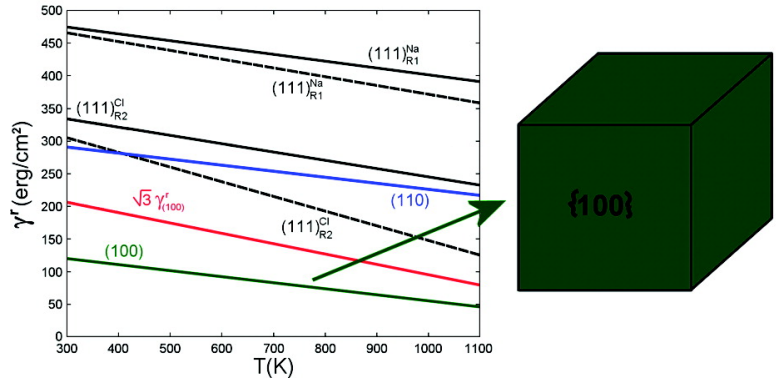

More About This Article

Additional resources and features associated with this article are available within the HTML version:

- Supporting Information
- Access to high resolution figures
- Links to articles and content related to this article
- Copyright permission to reproduce figures and/or text from this article

View the Full Text HTML

ACS Publications
High quality. High impact.

Crystal Growth and Design is published by the American Chemical Society. 1155 Sixteenth Street N.W., Washington, DC 20036

CRYSTAL GROWTH & DESIGN
2009
VOL. 9, NO. 4
1912–1916

Quantum-Mechanical and Thermodynamical Study on the (110) and Reconstructed (111) Faces of NaCl Crystals

Marco Bruno,* Dino Aquilano, and Mauro Prencipe

Dipartimento di Scienze Mineralogiche e Petrologiche, Università degli Studi di Torino, Via Valperga Caluso 35, I-10125 Torino, Italy

Received October 14, 2008; Revised Manuscript Received January 7, 2009

ABSTRACT: The (110) and R1 reconstructed (111) face (Na- or Cl-terminated) of halite (NaCl) were studied; the R1 reconstruction was performed by removing 50% of ions in the outermost layer of the face. The structures of the (110), $(111)^{Na}_{R1}$ and $(111)^{Cl}_{R1}$ surfaces were determined by means of ab initio quantum mechanical calculations (density functional theory, DFT). The $(111)_{R1}$ surfaces show higher surface relaxation with respect to the (110) surface. The surface energies (γ) at $T = 0$ K for relaxed and unrelaxed (110) and $(111)_{R1}$ faces were determined at DFT level. The values of the surface energy for the relaxed faces are: $\gamma_{(110)} = 330$, $\gamma_{(111)^{Na}_{R1}} = 520$ and $\gamma_{(111)^{Cl}_{R1}} = 530$ erg/cm^2; therefore, the stability order of relaxed surfaces reads (110) < $(111)^{Na}_{R1}$ < $(111)^{Cl}_{R1}$. For the unrelaxed faces the surface energies result to be higher: $\gamma_{(110)} = 387$, $\gamma_{(111)^{Na}_{R1}} = 825$ and $\gamma_{(111)^{Cl}_{R1}} = 769$ erg/cm^2; the stability order of the unrelaxed surfaces is (110) < $(111)^{Cl}_{R1}$ < $(111)^{Na}_{R1}$. To check if the $(111)_{R1}$ faces can belong to the equilibrium morphology of the crystal/vapor system, the relaxed surface energies at $T > 0$ K were calculated by considering both the vibrational motion of atoms and the surface configurational entropy. From these calculations it resulted that the $(111)^{Na}_{R1}$ and $(111)^{Cl}_{R1}$ faces cannot belong to the equilibrium morphology. Furthermore, it was also demonstrated that at room temperature the {110} and {111} forms cannot belong to the equilibrium shape of the NaCl crystal grown in pure aqueous solution. At equilibrium, the NaCl crystals can only show the {100} form.

Introduction

The halite (NaCl) crystal is cubic with space group *Fm*3*m* and $Z = 4$ (four formula units per cell); the lattice parameter is $a = 5.6401(2)$ Å at room temperature, as determined by X-ray diffraction measurements by Walker et al.[1] on synthetic NaCl powders.

The NaCl crystals obtained from vapor growth show exclusively the {100} form, while the morphology of NaCl crystals grown from aqueous solution is richer: in fact, {110} and {111} forms appear when a given amount of specific impurity (e.g., urea, formamide, $CdCl_2$) is added to the growth medium.[2,3] Moreover, some works reported that {111} NaCl faces can also be obtained from pure aqueous solution;[2,4,5] to the best of the authors knowledge, instead, no experimental observations of the {110} form was reported.

Crystals with NaCl structure consist of alternating layers of cations and anions stacked along the ⟨111⟩ directions. Therefore, the (111) surface is a polar one and must have a highly divergent electrostatic energy, which makes it unstable and not present in the equilibrium morphology. Therefore, to explain the presence of the {111} form in crystals with rocksalt-type structures grown from aqueous solution, the adsorption of impurities, H_2O molecules and/or H^+ and OH^- ions was invoked.[6,7] Instead, when no impurities are present, theoretical calculation suggests that the surfaces reconstruct.

To delete the macroscopic dipole moment, such reconstruction is performed by modifying the density of ions in the outermost layers of the crystal by the introduction of vacancies. Usually, this is done by moving charge from the outer planes of the stack to form new planes at the bottom. In practice, the macroscopic dipole moment is quenched by modifying the ionic density (or charge density) on the m outer planes according to the relation[8] $\sum_{j=1}^{m} \sigma_j = (-1)(\sigma_{m+1}/2)$, where σ_j is the charge density of the j-th plane. In our case, by applying this relation to the (111) slab, we can obtain two different surface reconstructions. The first one is performed by modifying the outer plane only (e.g., the plane containing the Na ions) of the slab: one-half of Na ions are moved from the outer plane of the (111) slab to a new plane at the bottom to produce a slab that is symmetrical about a central plane. In this way, the charge density of the latter plane (σ_1) equals half of the charge density of the second crystal plane ($\sigma_1 = -\sigma_2/2$). The same procedure is also valid when the outer plane of the slab is composed by Cl ions. The second type of surface reconstruction (octopolar reconstruction), which was originally suggested by Lacmann,[9] is performed by removing 75% of the ions in the outer layer of the slab and 25% of the ions in the underneath one; then, $\sigma_1 = \sigma_3/4$ and $\sigma_2 = -3\sigma_3/4$. As in the previous case, the octopolar (111) surfaces may be either Na or Cl terminated. In the following we will refer to these two surface reconstructions as R1 and R2 ones, respectively; we will use henceforth the notation $(111)^B_A$, where $A =$ R1 or R2, and $B =$ Na or Cl, to indicate the assumed different surface reconstructions and terminations.

Both of these reconstructions generate an electrically neutral slab, but only the {111} octopolar reconstructed surfaces respect the symmetry of the point group of the surface, being preserved the 3-fold axis perpendicular to the 111 plane. In a previous paper (Bruno et al.[10]), the relaxed structures of the $(111)^{Na}_{R2}$ and $(111)^{Cl}_{R2}$ faces, along with the (100) one, were determined at the DFT (density functional theory) level and their surface energies were calculated by considering both the vibrational motion of atoms (vibrational entropy) and the surface configurational entropy. According to these calculations, the octopolar {111} surfaces cannot enter the equilibrium morphology of crystals grown from vapor phase.

In this paper, we aim at obtaining detailed information on the structure of the (110), $(111)^{Na}_{R1}$ and $(111)^{Cl}_{R1}$ surfaces of NaCl crystals. We performed a quantum mechanical study of the structure of the (110), $(111)^{Na}_{R1}$ and $(111)^{Cl}_{R1}$ surfaces, whose geometries were optimized at the DFT level. Furthermore, to

* Corresponding author. E-mail: marco.bruno@unito.it. Tel.: 390116705131. Fax: 390116705128.

10.1021/cg801144x CCC: $40.75 © 2009 American Chemical Society
Published on Web 02/10/2009

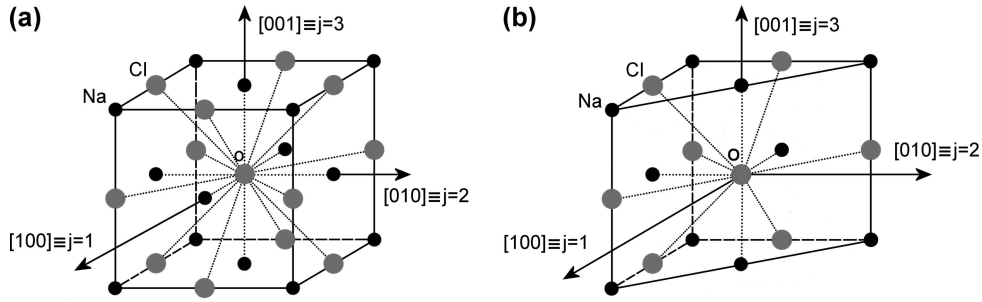

Figure 1. First nearest-neighbor atom polyhedron centered on the atom O in (a) the bulk crystal and (b) the (110) surface of NaCl. See text for details.

verify if the R1 reconstructed (111) face is more stable than the R2 reconstructed one, in crystals grown from vapor, the surface energies at $T \geq 0$ K of the $(111)^{Na}_{R1}$ and $(111)^{Cl}_{R1}$ surfaces, along with that of the (110) surface, were determined and compared with those of the $(111)^{Na}_{R2}$ and $(111)^{Cl}_{R2}$ faces. The surface energy at $T > 0$ K was calculated by taking into account both the vibrational entropy in the bulk and at its surface and the surface configurational entropy. Finally, we discuss the stability of the {110} and $\{111\}_{R1}$ forms in crystals grown from aqueous solution.

The study of the equilibrium morphology of NaCl crystals is a fundamental task, as many other strategic substances crystallize with the NaCl structure (e.g., MgO, NiO, ZnO, etc.) and the {0001} form of more complex ionic compounds, like calcite ($CaCO_3$), show exactly the same polarity problem of the {111} form of NaCl.[11]

Computational Details

Bulk and slab geometry optimizations were performed by means of the ab initio CRYSTAL06 code,[12] which implements the Hartree−Fock and Kohn−Sham, self-consistent field (SCF) method for the study of periodic systems.[13] The calculations were performed at DFT level; the B3LYP Hamiltonian[14] has been used, which contains a hybrid Hartree−Fock/density-functional exchange-correlation term. Details on the computational parameters are reported in Bruno et al.[10]

Geometry Optimization. Geometry optimizations (lattice parameters and fractional coordinates) of (110) and (111) slabs have been done for thickness up to ten and eight layers, respectively; lattice parameters and atomic coordinates of the ten-layer (110) and eight-layer (111) slabs are listed in Tables SI−SIII in the Supporting Information. We have ascertained that the considered thickness are sufficient either to reproduce bulklike properties at the center of the slabs, or to obtain an accurate description of the surfaces. Each slab of given thickness was generated by cutting the experimental bulk structure parallel to the face of interest [(110) and (111)], and by eliminating the atoms in excess, in the case of (111) face, in order to perform the R1 reconstruction.

The optimization of lattice parameters and atomic coordinates in the slab was performed by means of a modified conjugate gradient algorithm[15] as implemented in CRYSTAL06.[12]

Calculation of the Surface Energy at $T = 0$ K. The surface energy at 0 K [$\gamma(0)$] has been calculated by means of the following relation[16]

$$\gamma(0) = \lim_{n\to\infty} E_s(n) = \lim_{n\to\infty} \frac{E(n) - n[E(n) - E(n-1)]}{2A} \quad (1)$$

where A is the area of the primitive unit cell of the surface, and $E(n)$ is the energy of a n-layer slab; the factor 2 in the denominator accounts for the upper and lower surfaces of the slab. $E_s(n)$ is thus the energy per unit area required to form the surface from the bulk. As more layers are added in the calculation ($n \to \infty$), $E_s(n)$ will converge to the surface energy per unit area, $\gamma(0)$; ten- and eight-layer slabs are sufficient to reach convergence of the γ values for both the (110) and (111) faces.

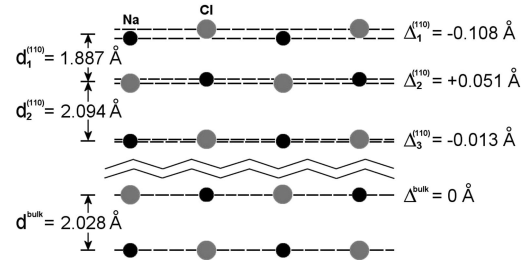

Figure 2. Schematic representation of the relaxed structure of the (110) slab viewed along the [$\bar{1}$10] direction.

Calculation of the Surface Energy at $T > 0$ K. The surface energy at temperatures higher than 0 K was calculated by taking into account the vibrational motion of atoms in the bulk crystal and that at its surface. We used the modified Kern's model, which is based on a monatomic Einstein crystal (for the derivation of the model, see Bruno et al.[10]). Such a model does not depend on the surface termination; no distinctions between Na- and Cl-terminated faces were done. The relation used to calculate $\gamma_\sigma(T)$, that is the surface energy of the face σ [(110), $(111)^{Na}_{R1}$ or $(111)^{Cl}_{R1}$] at temperature T, is the following

$$\gamma_\sigma(T) = \gamma_\sigma(0) + \frac{k_B\theta}{2}\sum_{k=1}^{p}\left\{ n_{k,\sigma}\sum_{j=1}^{3}\left[\left(\frac{\sum_{l=1}^{m_{k,\sigma}}(\cos\varphi_{k,l,j,\sigma})^2}{\sum_{l=1}^{m_b}(\cos\varphi_{l,j,b})^2}\right)^{\frac{1}{2}} - 1\right]\right\} + k_B T\sum_{k=1}^{p}\left[n_{k,\sigma}\ln\prod_{j=1}^{3}\left(\frac{\sum_{l=1}^{m_{k,\sigma}}(\cos\varphi_{k,l,j,\sigma})^2}{\sum_{l=1}^{m_b}(\cos\varphi_{l,j,b})^2}\right)^{\frac{1}{2}}\right] \quad (2)$$

where $\gamma_\sigma(0)$ is the surface energy at 0 K, $j = 1, 2, 3$ are three orthogonal axes lying along the 4-fold symmetry axes of the crystal ([100] $\equiv j =$ 1; [010] $\equiv j = 2$; [001] $\equiv j = 3$; Figure 1); $p = 1$ for the (110) face (Figure 1b), where every surface atom is coordinated by the same number of first neighbors ($m_{1,(110)} = 11$); $p = 2$ for the restructured (111) surface: its outermost layer ($k = 1$) contains only 50% of the available lattice sites with a coordination polyhedron formed by six atoms ($m_{1,(111)} = 7$); the layer below contain 100% ($k = 2$) of the sites with $m_{2,(111)} = 13$ (for an atom in the NaCl bulk, $m_b = 18$); $n_{k,\sigma}$ is the surface atomic density (atoms cm^{-2}) in the k-th layer of the surface σ; $\varphi_{k,l,j,\sigma}$ is the angle formed by the axis j and a vector $A_{k,l,\sigma}$-$O_{k,\sigma}$ joining an atom $O_{k,\sigma}$ in the k-th layer of the surface σ to an atom $A_{k,l,\sigma}$ of the first neighbor polyhedron centered on $O_{k,\sigma}$; $\varphi_{l,j,b}$ is the angle formed by the axis j and a vector joining an atom O_b in the bulk and an atom $A_{l,b}$ of the first neighbor polyhedron centered on O_b; k_B is the Boltzmann's constant; and θ is the Debye temperature of the solid ($\theta = 321$ K, for NaCl[17]).

The second term of eq 2 is the zero point energy (E^0_σ) of the surface σ. By considering unrelaxed surfaces, for the sake of simplicity, we calculated the following quantities to be inserted in eq 2

$$\sum_{l=1}^{m_b}(\cos\varphi_{l,1,b})^2=\sum_{l=1}^{m_b}(\cos\varphi_{l,2,b})^2=\sum_{l=1}^{m_b}(\cos\varphi_{l,3,b})^2=6$$

$$\sum_{l=1}^{m_{1,(110)}}(\cos\varphi_{1,l,1,(110)})^2=\sum_{l=1}^{m_{1,(110)}}(\cos\varphi_{1,l,2,(110)})^2=\frac{7}{2}\neq\sum_{l=1}^{m_{1,(110)}}(\cos\varphi_{1,l,3,(110)})^2=4$$

$$\sum_{l=1}^{m_{1,(111)}}(\cos\varphi_{1,l,1,(111)})^2=\sum_{l=1}^{m_{1,(111)}}(\cos\varphi_{1,l,2,(111)})^2=\frac{5}{2}\neq\sum_{l=1}^{m_{1,(111)}}(\cos\varphi_{1,l,3,(111)})^2=2 \quad (3)$$

$$\sum_{l=1}^{m_{2,(111)}}(\cos\varphi_{2,l,1,(111)})^2=\sum_{l=1}^{m_{2,(111)}}(\cos\varphi_{2,l,2,(111)})^2=4\neq\sum_{l=1}^{m_{2,(111)}}(\cos\varphi_{2,l,3,(111)})^2=5$$

Then, by using the surface densities (number of atoms/cm^2) $n_{1,(110)} = 8.89 \times 10^{14}$, $n_{1,(111)} = 3.14 \times 10^{14}$, and $n_{2,(111)} = 6.29 \times 10^{14}$, and the relaxed surface energy values at 0 K reported in Table 1, the surface energy at $T > 0$ K of the (110), $(111)^{Na}_{R1}$, and $(111)^{Cl}_{R1}$ faces can be calculated.

Results and Discussion

(110) Surface Structure. The (110) face of halite, observed along the [$\bar{1}$10] direction, is composed by electrically neutral layers. In Figure 2, the optimized (110) surface is reported. To describe the (110) slab structure, we used the following parameters[18]

$$\Delta_i^{(110)}=\frac{1}{2}(x_i^{Na}-x_i^{Cl}) \quad (4)$$

$$d_i^{(110)}=\frac{1}{2}(x_{i+1}^{Na}+x_{i+1}^{Cl}-x_i^{Na}-x_i^{Cl}) \quad (5)$$

where x_i^{Na} and x_i^{Cl} are the absolute coordinates along [110] of Na and Cl, respectively, in the i-th layer (for $i = 1,..., n$). $\Delta_i^{(110)}$ is the average rumpling of the i-th layer: it corresponds to the vertical dislocations of equal magnitude, but having opposite sign, of cations and anions out of the geometrical average of the layer. A positive (negative) rumpling is connected to an outward (inward) movement of the cations. $d_i^{(110)}$ is the average distance to the next underlying layer.

In the first layer, the Na cations are shifted inward, whereas the Cl anions are shifted outward ($\Delta_1^{(110)} = -0.108$ Å). In the underneath layers $\Delta_i^{(110)}$ converges rapidly to zero: $\Delta_2^{(110)} = 0.051$, $\Delta_3^{(110)} = -0.013$, and $\Delta_4^{(110)} = -0.001$ Å.

With reference to the $d_i^{(110)}$ parameter, the layer distance $d_1^{(110)} = 1.887$ Å is lower by ~10 and ~7% than those of the underneath layer ($d_2^{(110)} = 2.094$ Å) and bulk ($d^{bulk} = 2.028$ Å), respectively.

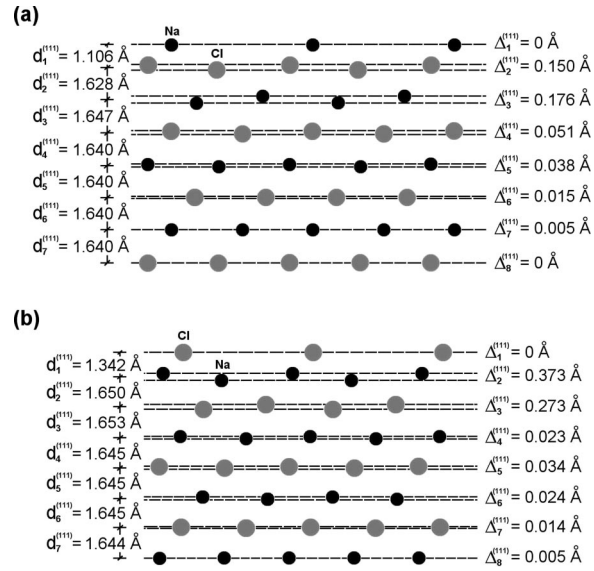

Figure 3. Schematic representations of the relaxed structures of the (a) $(111)^{Na}_{R1}$ and (b) $(111)^{Cl}_{R1}$ slabs viewed along a direction perpendicular to [111].

$(111)^{Na}_{R1}$and $(111)^{Cl}_{R1}$ Surface Structures. The (111) face of halite, observed along a direction perpendicular to [111], is composed by alternating layers of Na and Cl ions; in Figure 3 the optimized $(111)^{Na}_{R1}$ and $(111)^{Cl}_{R1}$ surfaces are reported. To describe the (111) slab structure,we used the following parameters[10]

$$\Delta_i^{(111)}=\frac{1}{2}(x_i^{h}-x_i^{l}) \quad (6)$$

$$d_i^{(111)}=\frac{1}{2}(x_{i+1}^{h}+x_{i+1}^{l}-x_i^{h}-x_i^{l}) \quad (7)$$

The meaning of such parameters is the same of those in eqs 4 and 5, but they are calculated by considering the absolute coordinates of the ions along [111] in the i-th layer; h and l indicate the highest and lowest ion (Na or Cl) in the i-th layer.

With reference to the $\Delta_i^{(111)}$ parameter, in both the surface terminations, $\Delta_1^{(111)} = 0$ by symmetry. The rumpling of the underneath layers of the $(111)^{Cl}_{R1}$ slab is higher with respect to that of the $(111)^{Na}_{R1}$ slab (Figure 3). As a matter of fact, $\Delta_2^{(111)} = 0.373$ and $\Delta_3^{(111)} = 0.273$ Å in the $(111)^{Cl}_{R1}$ slab, whereas $\Delta_2^{(111)} = 0.150$ and $\Delta_3^{(111)} = 0.176$ Å in the $(111)^{Na}_{R1}$ slab.

A large difference is noted in the layer distance $d_1^{(111)}$, which is 1.106 Å in the $(111)^{Na}_{R1}$ slab and 1.342 Å in the $(111)^{Cl}_{R1}$ slab, whereas no significant differences exist in the $d_i^{(111)}$ parameter of the underneath layers.

Surface Energies of (110), $(111)^{Na}_{R1}$, and $(111)^{Cl}_{R1}$ Faces. The resulting values of the relaxed surface energies (γ^r) at $T = 0$ K are reported in Table 1, along with the surface energies of the (100), $(111)^{Na}_{R2}$, and $(111)^{Cl}_{R2}$ faces calculated at DFT level by

Table 1. Relaxed, γ^r, and Unrelaxed, γ^u, Surface Energies at 0 K, And Zero Point Energies (E^0) of the (110), $(111)^{Na}_{R1}$, and $(111)^{Cl}_{R1}$ Faces; Surface Energies and Zero Point Energies of the (100), $(111)^{Na}_{R2}$ and $(111)^{Cl}_{R2}$ Faces Are Also Reported

	erg/cm^2				Kcal/(mol Å^2)				
	γ^r	γ^u	E^0	$\gamma^r + E^0$	γ^r	γ^u	E^0	$\gamma^r + E^0$	authors
(110)	330	387	−13	317	0.474969	0.557009	−0.018711	0.456258	this work
$(111)^{Na}_{R1}$	520	825	−14	506	0.748436	1.187423	−0.020150	0.728286	
$(111)^{Cl}_{R1}$	530	769	−14	516	0.762829	1.106822	−0.020150	0.742679	
(100)	160	161	−13	147	0.230288	0.231727	−0.018711	0.211577	Bruno et al.[10]
$(111)^{Na}_{R2}$	405	551	−17	388	0.582917	0.793054	−0.024468	0.558449	
$(111)^{Cl}_{R2}$	390	552	−17	373	0.561327	0.794494	−0.024468	0.536859	

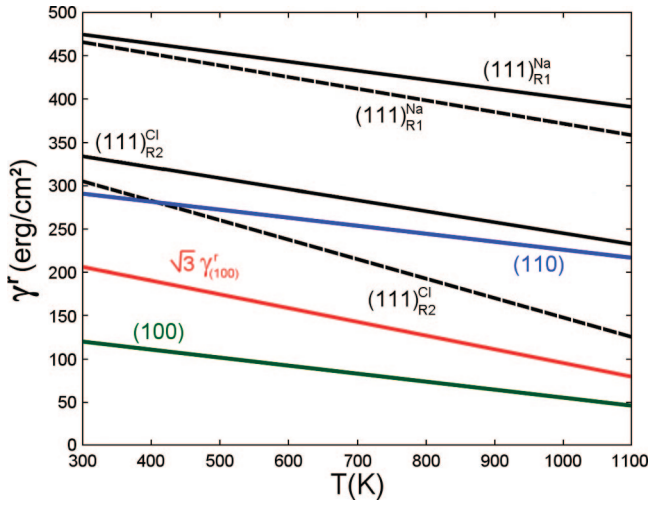

Figure 4. Surface energies of the (110) and $(111)^{Na}_{R1}$ faces reported as a function of temperature; the surface energies of the (100) and $(111)^{Cl}_{R2}$ faces are also reported (Bruno et al.[10]). Solid line, surface energies calculated without considering the configurational entropy; dashed line, surfaces energies calculated taking into account the configurational entropy.

Bruno et al.;[10] the stability order of the relaxed surfaces is (100) < (110) < $(111)^{Cl}_{R2}$ < $(111)^{Na}_{R2}$ < $(111)^{Na}_{R1}$ < $(111)^{Cl}_{R1}$. It is worth noting that in the case of the R1 reconstruction, the Na-terminated surface is more stable than the Cl-terminated one, whereas for the R2 reconstruction, the opposite is true. It is also interesting to observe that the zero point energy reduces the relaxed surface energies of the (110) and $(111)_{R1}$ faces by ~4 and ~3%, respectively (Table 1).

The surface energies for the unrelaxed faces (γ^u) have also been determined (Table 1); the relative stability order of the unrelaxed surfaces is (100) < (110) < $(111)^{Na}_{R2} = (111)^{Cl}_{R2}$ < $(111)^{Cl}_{R1}$ < $(111)^{Na}_{R1}$. According to these calculations, the octopolar reconstruction (R2) is favored with respect to the R1 reconstruction for both the relaxed and unrelaxed surfaces.

In the past, some estimates of the surface energy of the (110) face were obtained. Shi and Wortis,[19] by using empirical potentials (Born−Mayer−Huggins, BMH,[20] and Catlow−Diller−Norget, CDN,[21] potentials), obtained $\gamma^r_{(110)} = 307-425$ and $\gamma^u_{(110)} = 346-469$ erg/cm^2. The CDN potential was also used by Wolf,[22] who calculated for the relaxed and unrelaxed (110) faces $\gamma^r_{(110)} = 367-458$ erg/cm^2 and $\gamma^u_{(110)} = 384-472$ erg/cm^2, respectively. Finally, by considering a not-specified empirical potential, Mulheran[23] obtained $\gamma^r_{(110)} = 390$ erg/cm^2.

In the case of the $(111)_{R1}$ face, the only value of the surface energy at 0 K is given by Mulheran,[23] $\gamma^r_{(111)_{R1}} = 550$ erg/cm^2, which is in good agreement with our estimates (Table 1). It is important to underline that in the work by Mulheran[23] the $(111)_{R1}$ surface termination (Na or Cl) is not specified, whereas according to our calculations, differences of 56 and 10 erg/cm^2 are observed between the unrelaxed and relaxed $(111)^{Na}_{R1}$ and $(111)^{Cl}_{R1}$ surfaces, respectively.

The relaxed surface energies at $T > 0$ K (Figure 4) were calculated by using eq 2. We observe a decrease in ~100 erg/cm^2 for the $\gamma^r_{(110)}$ in the temperature range 0−1070 K (T_m = 1070 K, melting temperature of NaCl[24]), $((d\gamma)/(dT))_{(110)} = -0.091$ erg/(cm^2 K). This value is considerably lower than that obtained by Mulheran,[23] $((d\gamma)/(dT))_{(110)} = -0.04$ erg/(cm^2 K), by considering the correlation between the ionic vibrations.

In the same temperature range, the $\gamma^r_{(111)_{R1}}$ decreases in ~110 erg/cm^2, $((d\gamma)/(dT))_{(111)_{R1}} = -0.105$ erg/(cm^2 K). Such value is higher than that obtained by Bruno et al.[10] for the $(111)_{R2}$ surface, $((d\gamma)/(dT))_{(111)_{R2}} = -0.128$ erg/(cm^2 K).

To obtain a more accurate value of the surface energy, it is also necessary to determine the configurational entropy of the crystal face. In the case of the (110) surface, the contribution of the configurational entropy may be neglected, being this face similar to the (100) one, for which such a term is practically zero.[19,25] On the contrary, the configurational entropy is not negligible in the case of the $(111)_{R1}$ and $(111)_{R2}$ faces. An approximate estimate of $E^C_{(111)_{R2}}$, the surface configurational energy of the $(111)_{R2}$ face, is given by Shi and Wortis[19]

$$E^C_{(111)_{R2}} = -k_B T(0.323)\frac{\sqrt{3}}{d^2} \quad (8)$$

where d is the interionic distance (2.8102 Å). Following the approach of Shi and Wortis,[19] we also obtained a crude estimate of the surface configurational energy of the $(111)_{R1}$ face

$$E^C_{(111)_{R1}} = -k_B T n_{1,(111)} \ln 2 \quad (9)$$

As expected, the configurational entropy of the $(111)_{R2}$ face is significantly higher than that of the $(111)_{R1}$ surface, being $((E^C_{(111)_{R2}})/(E^C_{(111)_{R1}})) = 3.25$.

By considering eq 9, we calculated the surface energy of the $(111)_{R1}$ face (Figure 4). In the temperature range 0−1070 K, the configurational term causes a further decrease of ~30 erg/cm^2 in the surface energy of the $(111)_{R1}$ face; with the contribution of the configurational term, $((d\gamma)/(dT))_{(111)_{R1}}$ becomes −0.135 erg/(cm^2 K). On the whole, by taking into account (i) the vibrational motion of the atoms, (ii) the configurational energy and (iii) the zero point energy, the surface energy of the $(111)_{R1}$ face decreases by ~150 erg/cm^2; such a value is somewhat lower than that calculated by Bruno et al.[10] for the $(111)_{R2}$ face, ~250 erg/cm^2.

According to our calculations, the (110) and $(111)_{R1}$ faces cannot enter the equilibrium morphology of a NaCl crystal grown from vapor since, in the temperature range considered, the relations $\gamma_{(110)}(T) \le \sqrt{2}\gamma_{(100)}(T)$ and $\gamma_{(111)_{R1}}(T) \le \sqrt{3}\gamma_{(100)}(T)$ are never fulfilled (Figure 4).

{110} and {111} Forms in Crystals Grown from Aqueous Solution. In a recent work, Aquilano et al.[5] demonstrated that the $\{111\}_{R2}$ form cannot enter the equilibrium morphology of NaCl crystals grown from aqueous solution at $T = 300$ K. They established that the minimum energy of the $(111)_{R2}$ NaCl crystal−solution interface ($\gamma^{(111)_{R2}}_{cs} \approx 230$ erg/cm^2) is higher than $\sqrt{3}\gamma^{(100)}_{cs}$ ($\gamma^{(100)}_{cs} = 63$ erg/cm^2; the value of the (100) NaCl crystal−solution interfacial energy obtained from molecular dynamics simulation, MD, at pressure of 1 atm and $T = 300$ K, by Bahadur et al.[26]). $\gamma^{(111)_{R2}}_{cs}$ was calculated by using the Dupré's relation: $\gamma^{\sigma}_{cs} = \gamma^{\sigma}_{cv} + \gamma_{sv} - \beta^{\sigma}_{adh}$, where γ^{σ}_{cv} is the crystal-vapor interfacial energy, γ_{sv} is the specific surface energy between the NaCl saturated solution and the surrounding water vapor, and β^{σ}_{adh} is the adhesion energy between the surface σ of NaCl crystal and the surrounding saturated solution; $\gamma^{(111)_{R2}}_{cv} = 310$ erg/cm^2 (see Bruno et al.;[10] Figure 4), $\gamma_{sv} = 82$ erg/cm^2 (MD value by Bahadur et al.[26]), and $\beta^{(111)_{R2}}_{adh} = 2\gamma_{sv} = 164$ erg/cm^2 (it represents the highest value of the solid/liquid adhesion energy, because β^{σ}_{adh} cannot exceed the cohesion energy of the liquid, $2\gamma_{sv}$).

Similarly, we obtained the minimum values of $\gamma^{(111)_{R1}}_{cs}$ and $\gamma^{(110)}_{cs}$ at $T = 300$ K, by considering the highest value of the solid−liquid adhesion energy (164 erg/cm^2) and the crystal−vapor interfacial energies ($\gamma^{(111)_{R1}}_{cv}$ and $\gamma^{(110)}_{cv}$) determined in this work (Figure 4): $\gamma^{(111)_{R1}}_{cs}$ is 390 erg/cm^2, which is obviously higher

than $\gamma_{cs}^{(111)_{R2}}$, being $\gamma_{cv}^{(111)_{R1}} = 470$ erg/cm^2 > $\gamma_{cv}^{(111)_{R2}}$. Therefore, the $\{111\}_{R1}$ form cannot enter the equilibrium morphology of NaCl crystals grown from aqueous solution.

The minimum energy of the (110) NaCl crystal-solution interface at $T = 300$ K is $\gamma_{cs}^{(110)} \approx 210$ erg/cm^2; this value was calculated by using $\gamma_{cv}^{(110)} = 290$ erg/cm^2 (Figure 4). Accordingly, even the {110} form cannot enter the equilibrium morphology of NaCl crystals grown from aqueous solution, being $\gamma_{cs}^{(110)} > \sqrt{2}\gamma_{cs}^{(100)} \approx 90$ erg/cm^2.

Conclusions

The (110), $(111)_{R1}^{Na}$ and $(111)_{R1}^{Cl}$ slab optimizations of halite (NaCl) were performed at DFT level. The $(111)_{R1}^{Na}$ and $(111)_{R1}^{Cl}$ surfaces relax more than the (110) surface. As in the case of the (100) face,[10] the (110) surface shows small deviations from the bulk geometry: the Na shifted inward and Cl shifted outward with respect to the geometrical mean of the layer (Figure 2).

The surface energies at 0 K for relaxed and unrelaxed (110), $(111)_{R1}^{Na}$ and $(111)_{R1}^{Cl}$ faces, were determined at DFT level. By taking into account the surface energies of the (100), $(111)_{R2}^{Na}$ and $(111)_{R2}^{Cl}$ faces calculated at DFT level also,[10] the stability order is (100) < (110) < $(111)_{R2}^{Cl}$ < $(111)_{R2}^{Na}$ < $(111)_{R1}^{Na}$ < $(111)_{R1}^{Cl}$ for the relaxed surfaces and (100) < (110) < $(111)_{R2}^{Na} = (111)_{R2}^{Cl}$ < $(111)_{R1}^{Cl}$ < $(111)_{R1}^{Na}$ for the unrelaxed ones (Table 1).

The relaxed surface energies at 0 K of the $(111)_{R1}$ faces result to be significantly higher than those of the $(111)_{R2}$ faces. Such differences in the energy values suggests that the correct way to reconstruct the (111) surface of crystals with rocksalt-type structure is that proposed by Lacmann[9] (R2: octopolar reconstruction). Further, this is reasonable from the point of view of the bulk crystal symmetry, which cannot be arbitrarily interrupted at the crystal surface, as previously demonstrated by Massaro et al.[27] and Bruno et al.[28] for the (01.2) face of calcite. In fact, the only way to preserve the 3-fold axis perpendicular to the (111) surface is to consider the octopolar reconstruction, since any other reconstructed surface profile does not respect the crystal field imposed by the bulk.

The effect of temperature on relaxed surface energy was also taken into account. The surface energy at $T > 0$ K was calculated by considering the vibrational motion of atoms and the surface configurational entropy (Figure 4). According to our calculations, the (110) and $(111)_{R1}$ faces cannot belong to the equilibrium morphology of a NaCl crystal grown from vapor, as well as the $(111)_{R2}$ faces.[10]

Furthermore, we have demonstrated that at room temperature the {110} and {111} forms cannot belong to the equilibrium shape of the NaCl crystal grown in pure aqueous solution. Therefore, the occurrence[2,4,5] of the {111} form on the growth shape of the NaCl crystals in pure aqueous solution should be only due to a kinetic effect and, at equilibrium, the NaCl crystals can show only the {100} form.

Supporting Information Available: Tables listing the lattice parameters and atomic coordinates of the ten-layer (110) and eight-layer $(111)_{R1}$ slabs optimized at DFT level (PDF). This material is available free of charge via the Internet at http://pubs.acs.org.

References

(1) Walker, D.; Verma, P. K.; Cranswick, L. M. D.; Jones, R. L.; Clark, S. M.; Buhre, S. *Am. Mineral.* **2004**, *89*, 204–210.

(2) Kern, R. *Bull. Soc. Fr. Mineral Cristallogr.* **1953**, *76*, 391. (a) Bienfait, M.; Boistelle, R.; Kern, R. Adsorption et Croissance Cristalline. In *Colloques Internationaux du Centre National de la Recherche Scientifique* Kern, R., Ed.; Centre National de la Recherche Scientifique: Paris, 1965; Vol. 152, pp 515−535.

(3) Radenović, N.; van Enckevort, W.; Verwer, P.; Vlieg, E. *Surf. Sci.* **2003**, *523*, 307–315. (a) Radenović, N.; van Enckevort, W.; Vlieg, E. *J. Cryst. Growth* **2004**, *263*, 544–551. (b) Radenović, N.; van Enckevort, W.; Kaminski, D.; Heijna, M.; Vlieg, E. *Surf. Sci.* **2005**, *599*, 196–206.

(4) Johnsen, A. *Wachstum und Auflösung der Kristallen*;Engelmann: Leipzig, Germany, 1910.

(5) Aquilano, D. Pastero, L. Bruno, M. Rubbo, M. *J. Cryst. Growth* **2009**, *311*, 399−403.

(6) Rohr, F.; Wirth, K.; Libuda, J.; Cappus, D.; Bäumer, M.; Freund, H. J. *Surf. Sci.* **1994**, *315*, L977–L982. (a) Langell, M. A.; Berrie, C. L.; Nassir, M. H.; Wulser, K. W. *Surf. Sci.* **1994**, *320*, 25–38.

(7) Wander, A.; Bush, I. J.; Harrison, N. M. *Phys. Rev. B* **2003**, *68*, 233405.

(8) Duffy, D. M.; Harding, J. H. *Langmuir* **2004**, *20*, 7637–7642.

(9) Lacmann, R., Adsorption et Croissance Cristalline. In *Colloques Internationaux du Centre National de la Recherche Scientifique*; Kern, R., Ed.; Paris, France, 1965; Vol. 152, pp. 195−214.

(10) Bruno, M.; Aquilano, D.; Pastero, L.; Principe, M. *Cryst. Growth Des.* **2008**, *8*, 2163–2170.

(11) Pastero, L.; Costa, E.; Bruno, M.; Rubbo, M.; Sgualdino, G.; Aquilano, D. *Cryst. Growth Des.* **2004**, *4*, 485–490.

(12) Dovesi, R.; Saunders, V. R.; Roetti, C.; Orlando, R.; ZicovichWilson, C. M.; Pascale, F.; Civalleri, B.; Doll, K.; Harrison, N. M.; Bush, I. J.; D'Arco, Ph.; Llunell, M. *CRYSTAL06 User's Manual*; University of Torino: Torino, Italy, 2006.

(13) Pisani, C.; Dovesi, R.; Roetti, C. *Hartree−Fock Ab-Initio Treatment of Crystalline Systems, Lecture Notes in Chemistry*; Springer: Berlin, 1988.

(14) Becke, A. D. *J. Chem. Phys.* **1993**, *98*, 5648–5652.

(15) Civalleri, B.; D'Arco, Ph.; Orlando, R.; Saunders, V. R.; Dovesi, R. *Chem. Phys. Lett.* **2001**, *348*, 131–138.

(16) Dovesi, R.; Civalleri, B.; Orlando, R.; Roetti, C.; Saunders, V. R., Ab initio quantum simulation in solid state chemistry. In *Reviews in Computational Chemistry*; Lipkowitz, B. K., Larter, R., Cundari, T. R., Eds.; John Wiley & Sons: New York, 2005; Vol. 21, pp 1−125.

(17) Varshni, Y. P.; Konti, A. *J. Phys. C* **1972**, *5*, 2562–2566.

(18) Vogt, J.; Weiss, H. *Surf. Sci.* **2001**, *491*, 155–168.

(19) Shi, A. C.; Wortis, M. *Phys. Rev. B* **1988**, *37*, 7793–7805.

(20) Mayer, J. E. *J. Chem. Phys.* **1933**, *1*, 270–279.

(21) Catlow, C. R. A.; Diller, K. M.; Norgett, M. J. *J. Phys. C* **1977**, *10*, 1395–1412.

(22) Wolf, D. *Phys. Rev. Lett.* **1992**, *68*, 3315–3318.

(23) Mulheran, P. A. *Modell. Simul. Mater. Sci. Eng.* **1994**, *2*, 1123–1129.

(24) *Handbook of Chemistry and Physics*, 80th ed.; Lide, D. R., Ed.; CRC Press: Boca Raton, FL, 1999.

(25) Mayer, J. E. *J. Chem. Phys.* **1933**, *1*, 270–279.

(26) Bahadur, R.; Russell, L. M.; Alavi, S. *J. Phys. Chem. B* **2007**, *111*, 11989–11996.

(27) Massaro, F. R.; Pastero, L.; Rubbo, M.; Aquilano, D. *J. Cryst. Growth* **2008**, *310*, 706–715.

(28) Bruno, M.; Massaro, F. R.; Prencipe, M. *Surf. Sci.* **2008**, *602*, 2774–2782.

CG801144X